International Journal of Materials Science and Applications
2017; 6(5): 230-234
http://www.sciencepublishinggroup.com/j/ijmsa
doi: 10.11648/j.ijmsa.20170605.11
ISSN: 2327-2635 (Print); ISSN: 2327-2643 (Online)

Design for Stable Lasing of an Indirect Injection THz Quantum Cascade Laser Operating at Less Than 2 THz

Tsung-Tse Lin*, Hideki Hirayama

Terahertz Quantum Device Laboratory, Center for Advanced Photonics, RIKEN, Sendai, Japan

Email address:
ttlin@riken.jp (Tsung-Tse L.)
*Corresponding author

To cite this article:
Tsung-Tse Lin, Hideki Hirayama. Design for Stable Lasing of an Indirect Injection THz Quantum Cascade Laser Operating at Less Than 2 THz. *International Journal of Materials Science and Applications*. Vol. 6, No. 5, 2017, pp. 230-234. doi: 10.11648/j.ijmsa.20170605.11

Received: July 4, 2017; **Accepted**: July 17, 2017; **Published**: August 11, 2017

Abstract: In order to realize high temperature lasing of low frequency (< 2 THz) terahertz quantum cascade lasers (THz QCLs), selective carrier injection into an upper lasing level using an indirect injection (II) scheme is an effective method for inducing population inversion. The II scheme is realized with a four-level system. However, a three-level system that operates at low applied bias voltages causes additional lasing at higher frequencies (4～5 THz). By detuning the wave functions at the three lasing levels operating at low bias voltages, we were able to operate an II scheme THz QCL at a single stable frequency. Utilizing the higher injection selectivity, achieved through an indirect scattering-assisted injection process combined with diagonal emission, we were able to demonstrate stable operation of an AlGaAs/GaAs QCL operating at 1.89 THz at temperatures up to 160 K.

Keywords: Terahertz, Quantum Cascade Lasers, Indirect Injection

1. Introduction

The terahertz (THz) region in the electromagnetic spectrum has drawn much attention due to the wide range of applications available to this region, such as those in spectroscopy, imaging, remote sensing, and communications. Compact THz semiconductor sources are also extremely promising for use in future high-speed and large-capacity local telecommunications applications, especially for those applications operating in the range from sub-THz to a few THz (0.2 - 2 THz) [1]. High-output-power continuous-wave (cw) operation optical semiconductor devices are very attractive for overcoming this problem. Quantum cascade lasers (QCLs) [2] are compact semiconductor light sources that utilize carrier recycling and intersubband transitions in repeated quantum well (QW) structures, and they have been demonstrated to operate successfully in the mid-infrared (mid-IR) [2] and THz [3] regions. They are also arguably the only THz solid-state sources with average optical output power levels much greater than one milliwatt (mW) at pulse mode [4] and sub mW at CW operation [5]. This property of high optical output power with a narrow emission linewidth is quite attractive for a wide variety of THz applications [6].

In contrast to the room temperature operation of mid-IR QCLs, the maximum operating temperature (T_{max}) of THz QCLs is 199.5 K [7] at 3.2 THz. This performance was realized by an optimized state-of-the-art $Al_{0.15}Ga_{0.85}As$/GaAs structure utilizing longitudinal optical (LO) phonon depopulation for the extraction scheme with resonant tunneling (RT) injection and diagonal emission. The commonly reported high-temperature performance of THz QCLs roughly follows an empirical limitation depending on their operating frequency, such that $T_{max} \sim \hbar\omega/k_B$. Compared with the near 200 K operation of THz QCLs at 3 - 4 THz, at low frequencies (< 2 THz), THz QCLs are expected to exhibit poorer temperature performance due to this limitation when the frequency decreases. THz QCLs that operate at low frequencies suffer from design difficulties due to the narrow radiative energy separation between the two lasing-subband levels, which is related to the narrow dynamic range of the current density of the laser. Large thermal perturbation effects within the narrow energy level spaces have prevented the expansion of THz

QCLs to low-frequency high-temperature operation. This reduction in the dynamic range of the current density with operating frequency can be qualitatively explained by the dependence of the RT injection scheme on $k_B T_{max} \sim \hbar\omega$ [8]. It is known to be difficult to achieve both low frequency lasing and high-temperature operation.

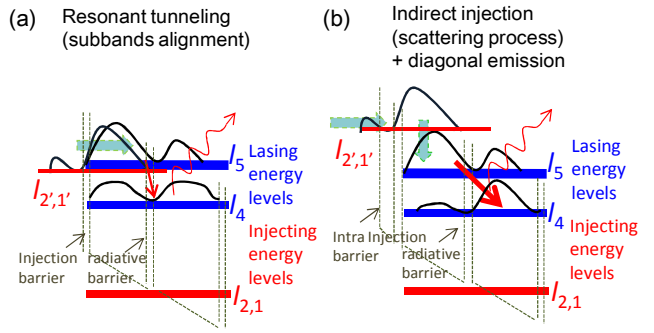

Figure 1. *Illustrative band-diagrams of (a) RT injection scheme with subband alignment and (b) Scattering-assisted II scheme with diagonal THz emission used in this work.*

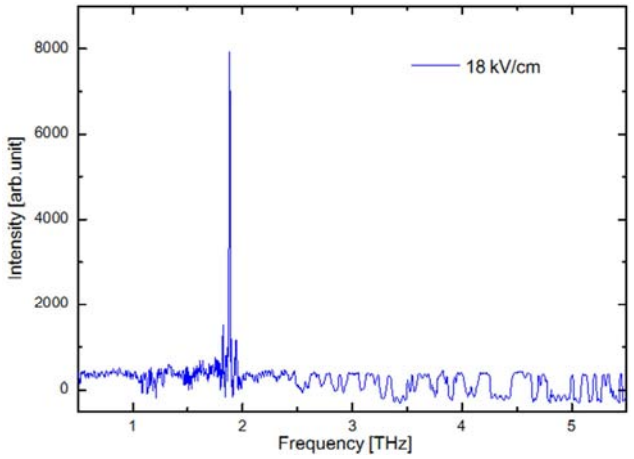

(a)

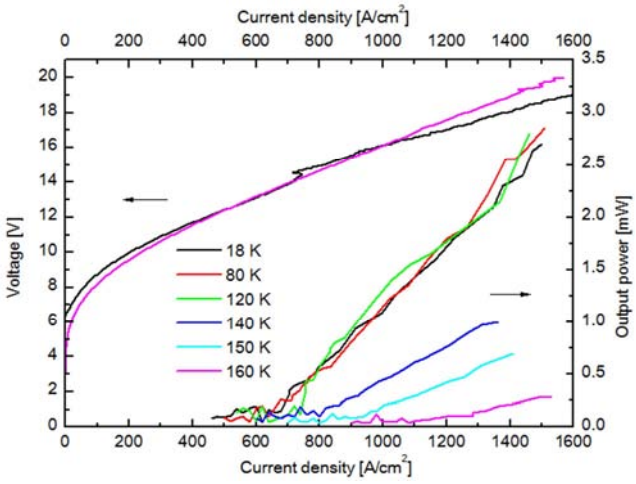

(b)

Figure 2. *(a) Laser emission spectrum (b) current density - light output (I-L) and current density - voltage (I-V) characteristics for various heat sink temperatures.*

A different kind of injection scheme, an indirect injection (II) scheme was first reported for mid-IR QCLs [9]. Illustrative band-diagrams of typical RT injection schemes are shown in figure 1(a) for a simplified 3-level system and an II scheme with diagonal THz emission in figure 1(b) for a simplified 4-level system, which is used in this work. Improvements in performance have been successfully achieved using fast and smooth LO phonon injection without carrier accumulation. The II scheme is also expected to circumvent the limitations of the RT injection scheme and to enable the realization of low-frequency THz QCLs operating at high temperatures. However, the much larger radiative energy in the mid-IR region causes different subband transport characteristics that need to be considered in the designs for THz frequencies. It is difficult to implement an II design with the correct carrier injection and narrow radiative energy at THz frequencies. Even this design scheme still suffers difficulties in the THz region compared with mid-IR QCLs. After several theoretical proposals [10, 11, 12], and a few recent experimental reports [8, 13, 14, 15, 16], II designs show promising results and demonstrate that there is high potential for attaining low-frequency, high-temperature THz QCLs.

2. Methods and Results

This work demonstrate an $Al_{0.175}Ga_{0.825}As$/GaAs QCL design that uses a combination of II and diagonal emission in the THz region. Structures were grown by solid-source molecular beam epitaxy (MBE); A 3.95 / 7.99 / 2.16 / 9.02 / 3.19 / 6.86 / 3.76 / 14.38 (nm) structure and 2.1×10^{16} cm^{-3} modulation doping of the widest well (14.38 nm) were employed. After MBE growth, the wafers were processed into Cu-Cu metal-metal waveguides (MMW) by Au-Au thermocompression wafer bonding. The 170 µm wide ridges of the laser bars were fabricated using photolithography and Cl_2 dry etching. Finally, we cleaved the laser bars with cavity lengths of 1.5 mm and measured them using a cryogenic Si-bolometer with an FT-IR system in pulsed mode. Figure 2(a) shows the measured emission spectrum at 5 K. Lasing is at 7.85 meV, corresponding to a frequency of 1.89 THz (wavelength of 158 µm). The observed emission energy was a little higher than the designed energy, possibly because the measured voltage was larger than the actual operating voltage due to the voltage drops at the Schottky contacts on either side of the MMW. Figure 2(b) shows the current density - light output characteristics (I-L curve) and the current density - voltage characteristics (I-V curve) of this QCL. The value of the threshold current density at low temperature was about 700 A/cm^2 with an output peak power in the range of a few mW, which was calibrated from the measurements made with the Si-bolometer. This THz QCL operated up to 160 K at a frequency of 1.9 THz, which is 1.8 times higher than the empirical temperature - frequency limitation of the conventional RT injection scheme.

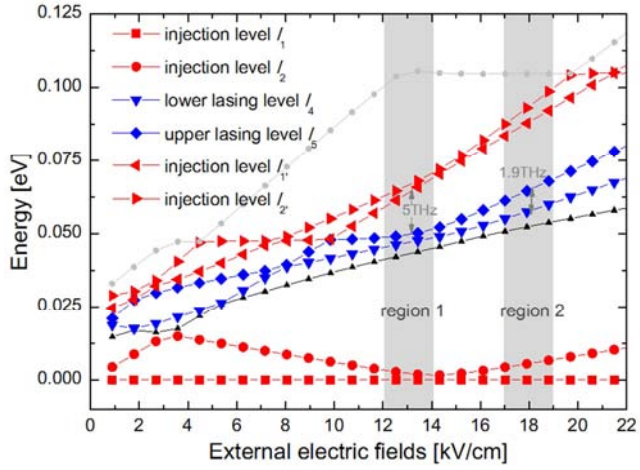

Figure 3. *Calculated energies of the subband levels in the band-diagram of the designed structure with respect to the external electric field. Region 1 is similar to conventional THz QCLs using the RT injection scheme, with a radiative energy of around 5 THz. Region 2 is for the II scheme combined with diagonal emission with radiative energy below 2 THz.*

3. Analysis of the Structure

3.1. General Operation of II THz QCLs

In practice, this kind of simplified 4-level II scheme depends very much on the external electric field. Figure 3 shows the dependence of the energy separation of the subbands on the external electric field for our structure. In the low electric field region around 12 - 14 kV/cm, the energy separation and band-diagram conditions are similar to the conventional RT injection scheme, such as shown in Figure 4(a): this shows a simplified 3-level-type design including two lasing levels and one injection level with a subband alignment injection process; the band-diagram related to this is shown in Figure 1(a). The injection process occurs from $l_{1'}$ (injection level at low bias) to $l_{2'}$ (upper lasing level at low bias) via an RT injection process. The emission frequency of about 5.0 THz (~ 20 meV) between $l_{2'}$ and l_5 (lower lasing level at low bias) is similar to the conventional RT injection lasing conditions. The first reported indirect type scattering-assisted (SA) injection QCLs in the THz region [8] also, initially, exhibited lasing at 4 THz. This emission occurred between similar subbands, $l_{2'}$ and l_5, to those in the RT injection scheme.

When the external electric field is increased, the mechanism between $l_{2'}$ and l_5 changes from a radiative process to an injection process by fast nonradiative thermally-activated LO phonon scattering. At higher electric fields, the LO phonon scattering process injects carriers and assists the targeted depopulation between l_5 and l_4 for emission at 1.8 THz. Here we reduced the thicknesses of the injection and emission barriers. Our design optimizes the energy separation between $l_{2',1'}$ and l_5, increasing it in order to approach the designed LO phonon energy. The fast nonradiative-injection scattering process between $l_{2',1'}$ and l_5 occurs earlier and restricts the low electric field emission to 4 - 5 THz. We also carefully optimized the wave functions between $l_{2'}$ to l_5, so that there is less overlap at low electric fields, with the related small oscillator strength reducing the possibility of lasing.

We focus only on the realization of a radiative process at high electric fields for 1.9 THz lasing. This occurs in the range of 17 - 19 kV/cm shown in Figure 3 and is related to the designed band-diagram in figure 4(b). Here we utilize the LO phonon scattering process to selectively-inject carriers from previous injection/extraction levels ($l_{2'}$, $_{1'}$) to the upper lasing level (l_5) indirectly. Then the LO phonon depopulation scheme extracts the carriers by fast LO phonon scattering from the lower lasing level (l_4) to the injection/extraction levels ($l_{2'}$, $_{1'}$) and injects the carriers into the next period of the cascade structure, in order to achieve population inversion within l_5 and l_4.

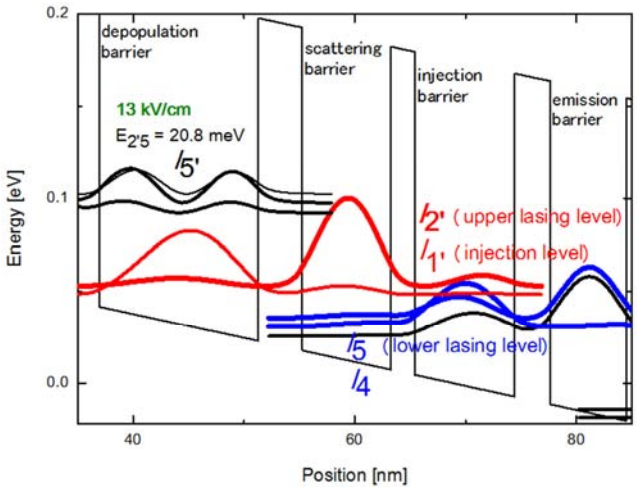

(a)

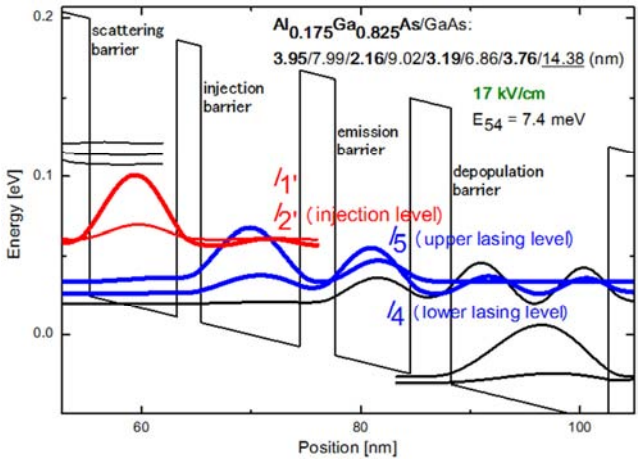

(b)

Figure 4. *Self-consistent calculations of the conduction band-diagrams of the $Al_{0.175}Ga_{0.825}As$/GaAs THz QCLs in two different external electric fields: (a) 13 kV/cm, (b) 17 kV/cm. The blue subbands are the designed lasing levels and the red ones are the injection levels for 1.9 THz emission.*

We calculated the relationship between the injection selectivity and the overlap between the wave functions of l_5 and l_4; as the spatial separation between the wave functions increases, the THz radiation changes from vertical to more

diagonal. The II selectivity from the injection level to the two lasing levels improves. If the LO phonon scattering relaxation time from $l_{2',1'}$ to l_5 is kept near 0.7 ps, and the wave function overlap ratio of f ($l_{2',1'}$, l_4)/f ($l_{2',1'}$, l_5) is changed from 0.9 (large overlap of l_5 and l_4) to 0.18 (small overlap of l_5 and l_4, which is used in this design), then the emission from l_5 to l_4 changes from vertical to diagonal. The relaxation time for the parasitic injection scattering from $l_{2',1'}$ to l_4 increases from 0.8 ps to 4 ps. It is the improvement in the injection selectivity by increasing the radiation diagonally that enables us to realize this II scheme in a THz QCL. Here it prefer to use thin high-Al content AlGaAs barriers [17, 18] in order to achieve an II scheme at THz frequencies with better injection selectivity by utilizing the diagonal emission design, and suppressing the high frequency emission at low bias (12 - 14 kV/cm) due to the simplified 3-level system.

3.2. Suppression of Unintentional Emission at Lower Bias and Enhancement of LO Phonon Scattering Assisted Indirect Injection

As mentioned before, previously reported works demonstrated unintentional lasing at lower bias in region I, shown in figure 3. In this work, we intentionally reduced the thickness of the scattering barrier. As a consequence, the tunneling transition from $l_{1'}$ to both l_2 and l_5 are enhanced, and thus the injection selectivity is lost if the barrier is thin enough. Therefore, population inversion becomes difficult to achieve. The results shown in figure 2 actually demonstrate that such unintentional lasing emission is not observed, as expected.

In parallel, we deliberately adopted a higher energy separation between $l_{2'}$ and l_5, compared to previous reports [8], namely, about 20.5 meV at 13KV/cm, and 30 meV at 18 KV/cm. With such a design, 30 meV is closer to the LO phonon energy, 36 meV. As a result, LO phonon scattering assisted indirect injection through the injection barrier in region II is significantly enhanced.

3.3. Enhancing the Designed 1.9 THz Emission by Optimizing the Injection and Emission Barriers

When the THz QCL operates at the target frequency, 1.9 THz, using the simplified 4-level II scheme with 17 - 19 kV/cm bias, the injection and emission barriers must be optimized for the best performance. The variation in oscillator strengths of the emission transition (l_5 to l_4) and injection transition ($l_{2'}$ to l_5) as a function of barrier thickness are shown in figure 5(a) and (b), respectively.

As shown in figure 5(a), a thinner injection barrier would increase the oscillator strength for the transition from $l_{2'}$ and l_5, which is once again improved. Therefore, the population in the upper lasing level l_5 is accumulated effectively, and helps to maintain population inversion, while the influence of such a thin injection barrier on the emission is not too serious.

The influence of the emission barrier thickness on the transition oscillator strength is shown in figure 5(b). The injection efficiency is almost constant in the range from 29 to 34 Å. In contrast, the emission is much enhanced when the emission barrier is made thinner.

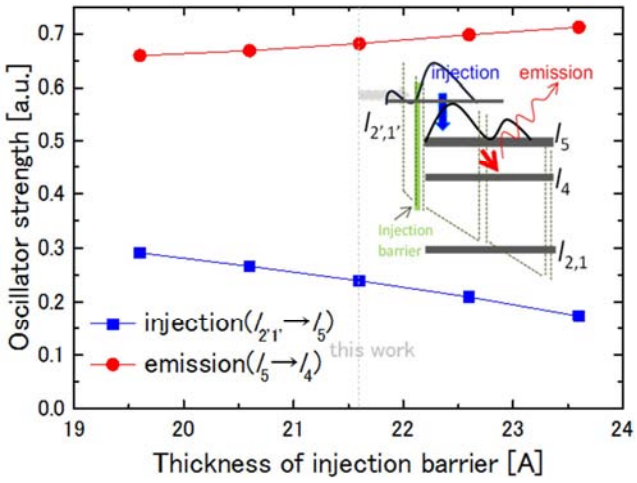

(a)

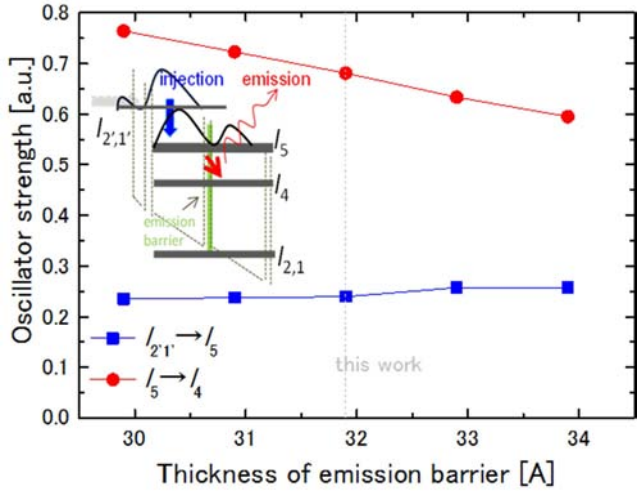

(b)

Figure 5. *Optimization of (a) injection barrier thickness and (b) emission barrier thickness with an external electric field of 17 kV/cm (region 1 in figure 3).*

3.4. Gain Calculation

The calculated maximum gain and emission photon energy at 150 K as a function of applied bias are shown in figure 6. The results are obtained by using the simulation software from Next Nano, which adopts the Non-Equilibrium Green's Function (NEGF) method. At relatively higher temperature, the results confirm that lasing at the target frequency can be obtained at around 2 THz. Moreover, the unintentional emission is effectively suppressed at lower bias.

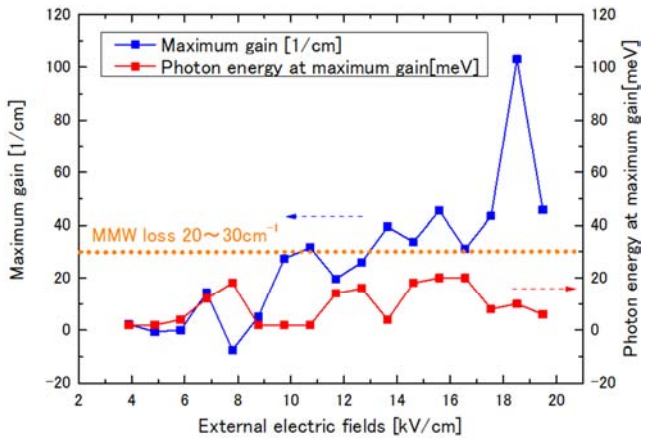

Figure 6. *Maximum gain and emission photon energy from the active region as functions of the external electric field calculated by the NEGF method. The typical loss of the MMW is around 20 ~ 30cm.*

4. Conclusion

In this paper, we have demonstrated a 1.9 THz $Al_{0.175}Ga_{0.825}As$/GaAs QCLs with T_{max} up to 160 K. The structure utilizes an indirect scattering process for injection and more diagonal THz emission. Moreover, this design has greater tolerance to both the electric field and thermal perturbations with a smooth current flow. We estimate this kind of II scheme has better selectivity relative to the correct level of injection with diagonal emission. With careful optimization of the wave functions with few specific barriers, we realized lasing restricted to frequencies below 2 THz.

References

[1] T. K.-Ostmann and T. Nagatsuma, "A Review on Terahertz Communications Research," J. Infrared. Milliw. TE. 32 (2011) 143.

[2] J. Faist, F. Capasso, D. L. Sivco, C. Sirtori, A. L. Hutchinson, and A. Y. Cho, "Quantum Cascade Laser," Science 264 (1994) 553.

[3] R. Köhler, A. Tredicucci, F. Beltram, H. E. Beere, E. H. Linfield, A. G. Davies, D. A. Ritchie, R. C. Iotti, and F. Capasso, "Terahertz semiconductor-heterostructure laser," Nature 417 (2002) 156.

[4] L. Li, L. Chen, J. Zhu, J. Freeman, P. Dean, A. Valavanis, A. G. Davies, and E. H. Linfield, "Terahertz quantum cascade lasers with >1 W output powers," Eectron. Lett. 50 (2014) 309.

[5] X. Wang, C. Shen, T. Jiang, Z. Zhan, Q. Deng, W. Li, W. Wu, N. Yang, W. Chu, and S. Duan, "High-power terahertz quantum cascade lasers with 0.23 W in continuous wave mode," AIP Advan. 6 (2016) 075210.

[6] G. Liang, T. Liu, and Q. J. Wang, "Recent Developments of Terahertz Quantum Cascade Lasers," IEEE j. sel. top. quantum electron 23 (2017) 1200118.

[7] S. Fathololoumi, E. Dupont, C. W. I. Chan, Z. R. Wasilewski, S. R. Laframboise, D. Ban, A. M´aty´as, C. Jirauschek, Q. Hu, and H. C. Liu, "Terahertz quantum cascade lasers operating up to˜200 K with optimized oscillator strength and improved injection tunneling," Opt. Express 20 (2012) 3866.

[8] S. Kumar, C. W. I. Chan, Q. Hu, and J. L. Reno, "A 1.8-THz quantum cascade laser operating significantly above the temperature of $h\omega/k_B$," Nat. Phys. 7 (2011) 166.

[9] M. Yamanishi, K. Fujita, T. Edamura, and H. Kan, "Indirect pump scheme for quantum cascade lasers: dynamics of electron-transport and very high T_0-values," Opt. Express 16 (2008) 20748.

[10] H. Yasuda, T. Kubis, P. Vogl, N. Sekine, I. Hosako, and K. Hirakawa, "Nonequilibrium Green's function calculation for four-level scheme terahertz quantum cascade lasers," Appl. Phys. Lett. 94 (2009) 151109.

[11] T. Kubis, S. R. Mehrotra, and G. Klimeck, "Design concepts of terahertz quantum cascade lasers: Proposal for terahertz laser efficiency improvements," Appl. Phys. Lett. 97 (2010) 261106.

[12] T. Liu, T. Kubis, Q. J. Wang, and G. Klimeck, "Design of three-well indirect pumping terahertz quantum cascade lasers for high optical gain based on nonequilibrium Green's function analysis," Appl. Phys. Lett. 100 (2012) 122110.

[13] E. Dupont, S. Fathololoumi, Z. R. Wasilewski, G. Aers, S. R. Laframboise, M. Lindskog, S. G. Razavipour, A. Wacker, D. Ban, and H. C. Liu, J. Appl. Phys. 111 (2012) 073111.

[14] K. Fujita, M. Yamanishi, S. Furuta, K. Tanaka, T. Edamura, T. Kubis, and G. Klimeck, "Indirectly pumped 3.7 THz InGaAs/InAlAs quantum-cascade lasers grown by metal-organic vapor-phase epitaxy," Opt. Express 20 (2012) 20647.

[15] S. G. Razavipour, E. Dupont, S. Fathololoumi, C. W. I. Chan, M. Lindskog, Z. R. Wasilewski, G. Aers, S. R. Laframboise, A. Wacker, Q. Hu, D. Ban, and H. C. Liu, "Delay time calculation for dual-wavelength quantum cascade lasers," J. Appl. Phys. 113 (2013) 203107.

[16] S. Khanal, J. L. Reno, and S. Kumar, "2.1 THz quantum-cascade laser operating up to 144 K based on a scattering-assisted injection design," Opt. Express 23 (2015) 19689.

[17] T.-T. Lin, L. Ying, and H. Hirayama, "Threshold Current Density Reduction by Utilizing High-Al-Composition Barriers in 3.7 THz GaAs/Al_xGa_{1-x} As Quantum Cascade Lasers," Appl. Phys. Express 5 (2012) 012101.

[18] T.-T. Lin and H. Hirayama, "Improvement of operation temperature in GaAs/AlGaAs THz-QCLs by utilizing high Al composition barrier," Phys. Stat. Sol. C 10 (2013) 1430.